Toxicology Reports 2 (2015) 472–481

Contents lists available at ScienceDirect

Toxicology Reports

journal homepage: www.elsevier.com/locate/toxrep

Craniofacial form is altered by chronic adult exposure to 2,3,7,8-tetrachlorodibenzo-*p*-dioxin (TCDD) in Han/Wistar and Long–Evans rats with different aryl hydrocarbon receptor (AhR) structures

Sabrina B. Sholts[a,*], Javier Esteban[b], Maria Herlin[c,d], Matti Viluksela[e,f], Helen Håkansson[d]

[a] *Department of Anthropology, National Museum of Natural History, Smithsonian Institution, 10th and Constitution Avenue NW, Washington, DC 20560, USA*
[b] *Instituto de Bioingeniería, Universidad Miguel Hernández, Av. de la Universidad s/n, 03202 Elche (Alicante), Spain*
[c] *Clinical and Molecular Osteoporosis Research Unit, Department of Clinical Sciences, Lund University, Inga Marie Nilssons gata 22, SE-22100 Lund, Sweden*
[d] *Institute of Environmental Medicine, Karolinska Institutet, P.O. Box 210, SE-17177 Stockholm, Sweden*
[e] *Department of Environmental Health, National Institute for Health and Welfare, P.O. Box 95, FI-70701 Kuopio, Finland*
[f] *Department of Environmental Science, University of Eastern Finland, Kuopio, Finland*

ARTICLE INFO

Article history:
Received 12 December 2014
Accepted 12 December 2014
Available online 19 December 2014

Chemical compounds studied in this article:
2,3,7,8-Tetrachlorodibenzo-*p*-dioxin (PubChem CID: 15625)

Keywords:
2,3,7,8-Tetrachlorodibenzo-*p*-dioxin
Bone
Toxicology
Cranial morphology: Geometric morphometrics
Aryl hydrocarbon receptor

ABSTRACT

Mammalian bone has shown a variety of responses to 2,3,7,8-tetrachlorodibenzo-*p*-dioxin (TCDD) exposure in experimental and wildlife studies. Although many responses have been well characterized in the postcranial skeleton, dioxin-induced effects on the cranium are largely unknown. In this study, we investigated the effects of chronic adult exposure to TCDD on cranial size and shape in dioxin-resistant Han/Wistar (H/W) and dioxin-sensitive Long–Evans (L–E) rat strains. Three-dimensional landmark configurations for the face, vault, and base of the cranium were recorded and analyzed using geometric morphometrics (GM) and dose–response modeling. The strongest effects were shown by L–E and H/W rats with daily exposures of 100 and 1000 ng TCDD/kg bw/day, respectively, resulting in significant reductions in centroid size (CS) in all three cranial modules for both strains except for the vault in H/W rats. Consistent with previous evidence of intraspecific variation in TCDD resistance, the benchmark doses (CEDs) for cranial size reduction in L–E rats were roughly 10-fold lower than those for H/W rats. For both strains, the face showed the greatest size reduction from the highest doses of TCDD (i.e., 3.6 and 6.3% decreases in H/W and L–E rats, respectively), most likely related to dose-dependent reductions in limb bone size and body weight gain. However, intrinsic morphological differences between strains were also observed: although the control groups of H/W and L–E rats had vaults and bases of comparable size, the face was 6.4% larger in L–E rats. Thus, although H/W rats possess an altered aryl hydrocarbon receptor (AhR) that appears to mediate and provides some resistance to TCDD exposure, their smaller reductions in facial size may also relate to strain-specific patterns of cranial development and growth. Future research will be aimed at understanding how ontogenetic factors may modulate toxic effects of prenatal and lactational exposure on the mammalian skeleton.

* Corresponding author.
E-mail addresses: sholtss@si.edu (S.B. Sholts), jesteban@umh.es (J. Esteban), maria.herlin@med.lu.se (M. Herlin), matti.viluksela@thl.fi (M. Viluksela), Helen.Hakansson@ki.se (H. Håkansson).

http://dx.doi.org/10.1016/j.toxrep.2014.12.007

1. Introduction

Exposure to persistent organic pollutants (POPs) is a major worldwide health concern. Although production of some POPs has been banned for decades, exposures can still result from past uses, improper disposal practices, accidents, and unregulated production in developing countries [1]. Once introduced into the environment, POPs degrade slowly and undergo cycling and transport within the various compartments of the global ecosystem, where they can be taken up and stored by species at all trophic levels of a food chain [2–4]. Understanding the toxicological mechanisms and potential adverse biological effects of these chemicals is thus important for accurately assessing and predicting human and animal health risks from exposure.

In general, POPs are associated with a wide range of adverse biological effects, including immunotoxicity, neurotoxicity, hepatoxicity, and tumor promotion [5]. As endocrine-disrupting compounds (EDCs), many of these chemicals have also the ability to interfere with hormonal programming and regulation of growth and development in exposed organisms [6]. For POPs such as dioxins, a highly toxic group of chlorinated hydrocarbons, practically all adverse effects are mediated by the aryl hydrocarbon receptor (AhR). Among its many functions, the AhR appears to play an essential role in the differentiation and maturation of the osteoclasts and osteoblasts that form and maintain bone [7], which can be disrupted when dioxins bind to the AhR protein [8]. The magnitude of toxic potency of individual dioxin-like compounds is estimated as a toxic equivalency factor (TEF) in relation to 2,3,7,8-tetrachlorodibenzo-*p*-dioxin (TCDD), the model compound and the most toxic member of the dioxin group [9].

Mammalian bone has shown a variety of responses to TCDD exposure in experimental and wildlife studies. In the postcranial skeleton, TCDD exposure has been associated with significant alterations in bone mineral density, biomechanical strength, and bone geometry among different rat strains and at dose levels of relevance to human and wildlife exposure situations [10–13]. In the skull, dioxin-induced changes in the size and shape of the mandible of exposed mice have been identified using geometric morphometric techniques [14,15]. Teeth also exhibit dioxin sensitivity, as low levels of in utero/lactational exposure and high levels of adult exposure have shown numerous effects on eruption, size, structure, and caries susceptibility [16–19]. However, with the exception of specific developmental defects such as cleft palate [20–23], the effects of dioxins on cranial formation have not been extensively studied. It has been shown that a single dose of TCDD can impair normal cranial growth in young adult male Han/Wistar rats [16], yet it is unclear how responses may vary among different strains, exposure levels/periods, and cranial traits or modules. Given that cranial form plays a key role in the protection and structural support for many vital organs and sensory functions, in addition to its taxonomic, phylogenetic, and anthropological significance, this information has broad relevance across the life sciences.

In this study, we investigated the effects of chronic TCDD exposure on cranial size and shape in the adult female rats of two different strains, Han/Wistar (H/W) and Long–Evans (L–E). H/W rats are exceptionally resistant to many endpoints of dioxin toxicity due to a truncated AhR transactivation domain, while L–E rats express the wild-type AhR [24,25]. In order to cover the whole spectrum of biological effects observed in both strains [11–13,26], the experimental treatments ranged from high to low (human relevant) doses. Using geometric morphometrics (GM), the crania of these rats were analyzed as three morphological modules (i.e. face, vault, and base) that have previously shown differential effects of growth reduction from environmental stress in rats [27]. Building on previous work showing cranial size reduction in rats resulting from early adult exposure [16], this approach allowed us to identify specific cranial traits and growth processes affected by TCDD exposure, providing new information and a fuller understanding about dioxin and dioxin-like effects on the mammalian skeleton.

2. Materials and methods

2.1. Animals and treatments

The experimental protocol, including animal housing and care, was approved by the Animal Experiment Committee at the University of Kuopio and the Kuopio Provincial Government in Finland (for details, see [26]). Ten-week-old female H/W (Kuopio) and L–E (Turku/AB) rats were administered TCDD in corn oil by s.c. injection (2 ml/kg) once per week for 20 weeks; control rats received corn oil only. All rats were weighed weekly from birth until week 25 [26] (Fig. 1). To achieve rapidly the kinetic steady state, in order to mimic adult human steady-state exposure, the first treatment was a loading dose 5 times higher than the 19 subsequent weekly maintenance doses [28]. The total doses were 0, 0.17, 1.7, 17 μg (both strains) and 170 μg (H/W only) TCDD/kg bw. The daily doses were 0, 1, 10, 100, and 1000 ng TCDD/kg bw, respectively. Exposure at the low dose, i.e. 1 ng TCDD/kg bw, resulted in animal tissue levels comparable to the concentrations of polychlorinated dibenzo-*p*-dioxins (PCDD) and dibenzofurans (PCDF) observed in humans at background exposure levels [12,26], which makes the applied dose levels and obtained study results relevant to human health risk assessment.

2.2. Data collection

The heads from a total of 90 rats (10 per dose group) were dissected and frozen before being skinned and then skeletonized by dermestid beetles. On each of the skeletonized crania, the locations of 47 three-dimensional (3D) landmarks were identified and marked by pencil (Table 1). The number of selected landmarks was determined by the size and complexity of the face ($n = 23$), vault ($n = 8$), and base ($n = 16$) (Fig. 2). Numerous studies have shown that the precision with which landmarks can be located varies between different types of landmarks, such as those at sutural intersections (Type 1), those at geometric maxima of bony protrusions or depressions (Type 2), and those at extreme locations with respect to other landmarks or geometric entities (Type 3) [29]. For landmark measurements on the skull, 3D digitizers have shown the highest

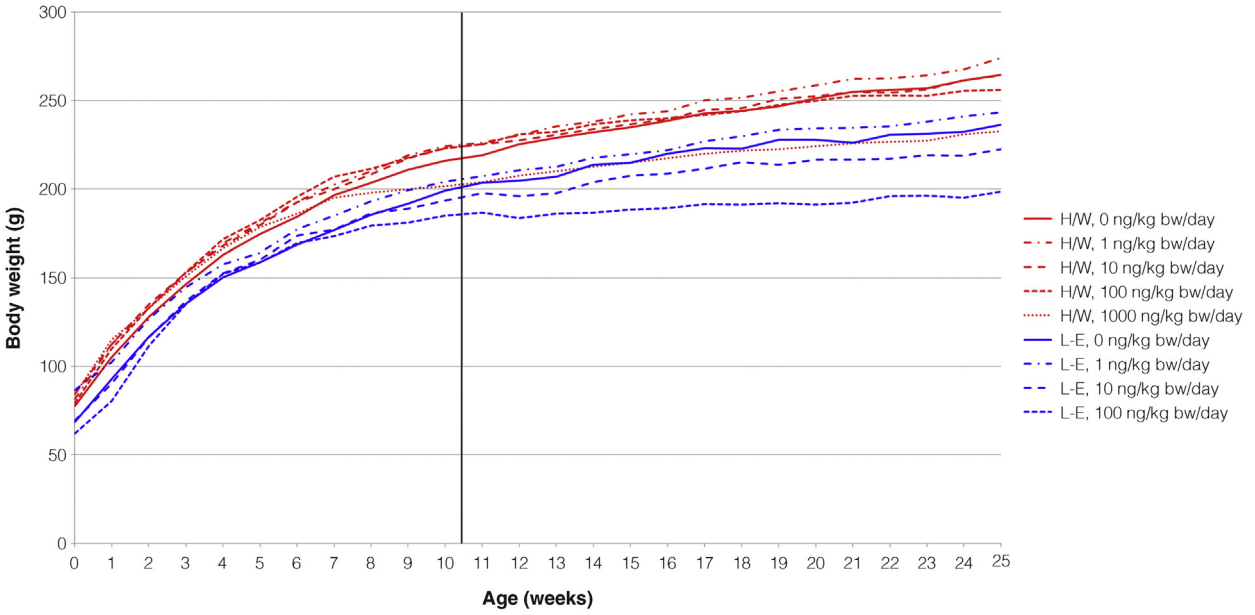

Fig. 1. Body weight (g) of female Han/Wistar (H/W) and Long–Evans (L–E) rats in the study sample at 1 to 25 weeks of age. Lines are color-coded by strain (Han/Wistar = red, Long–Evans = blue) and patterned by dose group (control = solid, 1 ng/kg bw/day =dash-dot, 10 ng/kg bw/day =long dashes, 100 ng/kg bw/day =small dashes, and 1000 ng/kg bw/day =dots).

Table 1
Landmarks measured in this study.

Module	Paired	Landmark definition
Face	x	Anteriormost nasal–premaxilla intersection
	x	Anteriormost point on maxilla
	x	Point of deepest lateral incurvature on the superior aspect of the infra-orbital fissure
	x	Frontal–premaxilla–maxilla intersection
	x	Frontal–premaxilla–nasal intersection
		Nasion (frontal–frontal–nasal–nasal intersection)
	x	Frontal–lacrimal–maxilla intersection
	x	Anteriormost premaxilla–premaxilla intersection between the incisors
	x	Inferiormost premaxilla–premaxilla intersection between the incisors
	x	Anteriormost margin of incisive foramen
	x	Point of deepest posterior incurvature on the inferior aspect of the infra-orbital fissure
	x	Posteriormost margin of incisive foramen
	x	Lateral alveolar margin superior to second molar at the midpoint of anteroposterior length
Vault	x	Medial point on the temporal line at the frontal–parietal intersection
		Bregma (intersection at the coronal and sagittal sutures)
	x	Point of deepest posterior incurvature on the anterior aspect of the squamosal bone
		Lambda (parietal–parietal–interparietal intersection)
	x	Medial point on the temporal line at the parietal–interparietal intersection, left
Base		Superiormost point on the posterior margin of the foramen magnum
	x	Lateralmost point on the posterior margin of the foramen magnum
		Anteriormost point on the inferior margin of the foramen magnum
	x	Point of deepest posterior incurvature on the anterior aspect of the paraoccipital process
	x	Lateralmost point on the perotic capsule
	x	Occipital–auditory–sphenoid intersection
	x	Anteriormost point on the inferior margin of the foramen ovale
	x	Lateral palatal–pterygoid intersection
		Posterior palatine–palatine intersection
		Anterior palatine–palatine intersection

precision for Type 1 landmarks and the lowest for Type 3 [30–33]. In order to minimize the potential for measurement error, only Type 1 and Type 2 landmarks were used in this study. With the cranium fixed in a stable position, the marked landmark locations were recorded digitally as 3D coordinates with a Microscribe G2X system (Revware Systems, Inc., 2009) by the same recorder in two trials on different days. In the few cases where fractured or missing bone did not permit landmark measurement, the specimen was omitted from the sample.

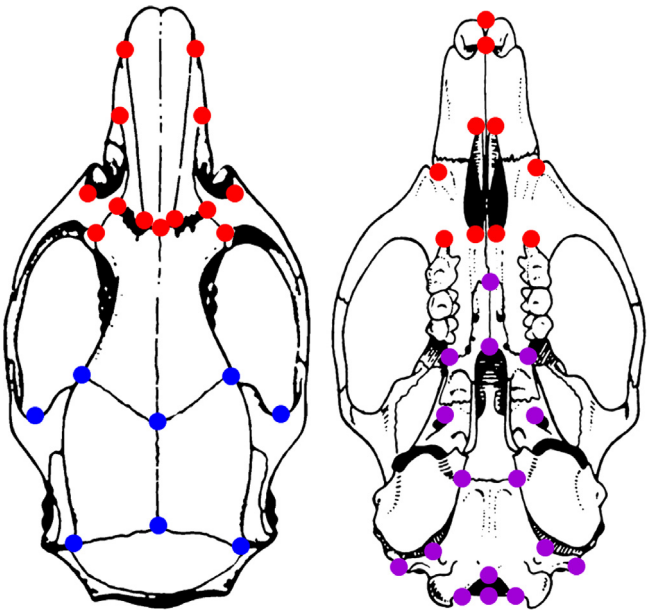

Fig. 2. Landmarks measured on crania of female Han/Wistar (H/W) and Long–Evans (L–E) rats in the study sample. Landmarks are color-coded by cranial module (face = red, vault = blue, base = purple). Drawings are modified from Vinogradov and Argiropulo [57].

2.3. Geometric morphometrics (GM)

Complete landmark configurations from a total sample of 83 crania were scaled, rotated, and translated by means of generalized least-squares Procrustes superimposition with MorphoJ version 1.06b software [34]. The initial Procrustes fit was performed on all configurations of all 47 landmarks for measurement error analysis, after an initial check for outliers. Following Jamniczky and Hallgrímsson [35], principal components analysis (PCA) and discriminant function analysis (DFA) were used to assess intra-observer error between the two trials. The PCA showed no differences in distribution (Fig. 3), and the DFA classified observations by measurement trial with relatively low accuracy (63% with cross-validation). Both measurement trials were averaged by individuals for all subsequent analyses.

To assess shape variation in the sample, PCA was performed on shape data resulting from a Procrustes fit for the entire set of 47 landmarks, combining all three cranial modules. As the majority of landmarks in the configurations were paired (i.e., bilateral), only the symmetric component of total shape variation (i.e., the averaged Procrustes coordinates of each specimen and its mirrored image) was analyzed (see [36]). This approach provided a graphical display of shape changes in individual landmark configurations relative to the consensus shape, showing which aspects of shape accounted for the greatest amount of variation.

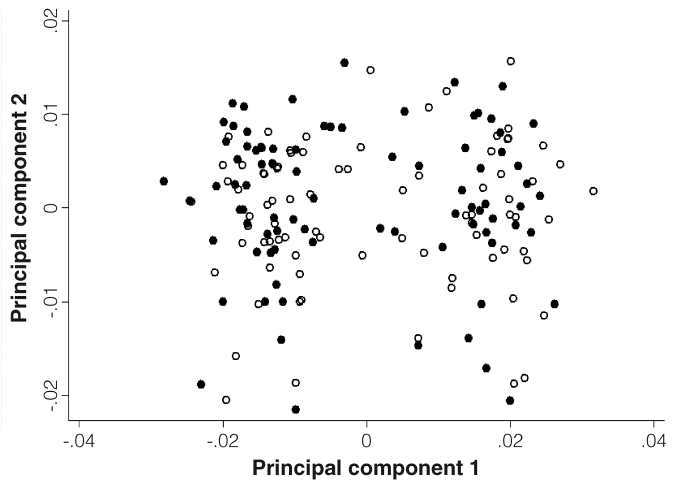

Fig. 3. Principal components analysis (PCA) of intra-observer landmark measurement error. Score plot for the first two PCs derived from the symmetric component of the Procrustes shape coordinates for all 47 landmarks in two measurement trials for the study sample. Markers are symbol-coded by trial (trial 1 = filled circle, trial 2 = hollow circle).

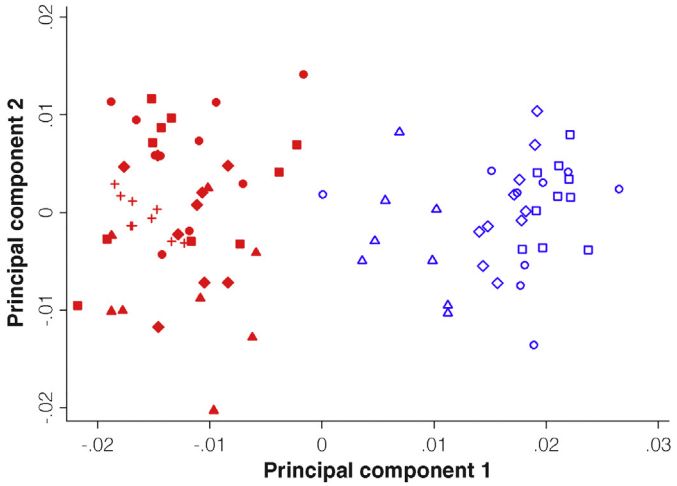

Fig. 4. Principal components analysis (PCA) of overall cranial shape variation in female Han/Wistar and Long–Evans rats in the study sample. Score plot for the first two PCs derived from the symmetric component of the Procrustes shape coordinates of all 47 landmarks. Markers are color-coded by strain (Han/Wistar = red, Long–Evans = blue) and symbol-coded by dose group (control = circle, 1 ng/kg bw/day =square, 10 ng/kg bw/day =diamond, 100 ng/kg bw/day =triangle, and 1000 ng/kg bw/day =plus).

To assess size variation in the sample, Procrustes fits were performed separately on the three subsets of landmarks for the face, vault, and base. The resulting dataset from each Procrustes fit included a standard size variable of centroid size (CS), defined as the square root of the sum of squared distances of a set of landmarks from their centroid. Data were evaluated with the Shapiro-Wilk test for normality and Levene's test for homogeneity of variance, and failed to meet parametric assumptions. Non-parametric test statistics of Wilcoxon's rank sum and Spearman's rank correlation coefficient (r_S) were thus used for comparisons between the CS values and other measurements of postcranial size and body weight for different dose groups and strains. All CS analyses were performed with Stata version 10 statistical software (StataCorp LP 2007).

2.4. Dose–response modeling

A family of exponential models (PROAST version 38.9 [RIVM, Bilthoven, The Netherlands] in the R software version 3.1.0, [R Development Core Team, R Foundation for Statistical Computing, Vienna, Austria]) was used for dose–response modeling of CS values of the face, base, vault, and overall cranium. Based on the likelihood ratio test, the appropriate model was fitted to the data acquired from each strain. The benchmark dose (critical effect dose, CED) was calculated at a change of one standard deviation of the response in unexposed subjects [37]. Furthermore, CED at the lower bound of the associated 95% confidence interval (CED-L5) was computed as well as the CED/CED-L5 ratio [38].

3. Results

Overall cranial shape variation in the sample is shown by the PCA score plot in Fig. 4. More than one-third of the total variation (i.e., 35%) is described by the first principal component (PC 1), which shows a clear separation of the H/W and L–E strains by negative and positive scores, respectively. In Fig. 5, the shape changes that correspond to a positive change in PC 1 score by 0.1 units are illustrated with a lollipop graph, which visualizes the location and magnitude of these changes as lines extending from the landmark locations in the consensus configuration. As indicated by the long lines in the face component, the most extreme PC 1 shape changes were the anterior–posterior displacement of landmarks around the nasal and maxillary bones. By comparison, the maximum dimensions of the vault and base modules were largely unchanged. These results showed that L–E rats in general had larger and longer faces than H/W rats relative to the rest of the cranium. Within the L–E strain, the rats with the highest level of TCDD exposure had the lowest PC 1 scores, indicating reduced facial size in this group (Fig. 4). Among the H/W rats, strong dose-related patterns in cranial shape were not evident (Fig. 4).

Size variation in the sample is shown by differences in CS values, which are reported as mean ± standard deviation (SD) in Table 2 and as box plots in Fig. 6. Dose–response relationships were found for all CS datasets according to ANOVA and dose–response modeling, with the exception of the H/W vault (Table 3). In L–E rats, all three cranial modules were reduced (Table 2), i.e., face with a CED of 5.9 μg/kg bw (maximal response of 6.4%), vault with a CED of 0.0017 μg/kg bw (maximal response of 1.9%), and base with a CED of 6.7 μg/kg bw (maximal response of 3.4%) (Table 3). In H/W rats, CS values were reduced (Table 2) for the face with a CED of 78 μg/kg bw (maximal response of 3.8%) and for the base with a CED of 73 μg/kg bw (maximal response of 3.2%) (Table 3). Due to these differences between H/W and L–E rats, CS values for the face and the overall cranium showed a strong positive correlation within each strain ($r_S = 0.90$ and 0.95, $p < 0.001$) and no correlation when the strains were combined ($r_S = 0.58$, $p < 0.001$) (Table 4). In contrast, base size was strongly positively correlated with overall cranial size both within and

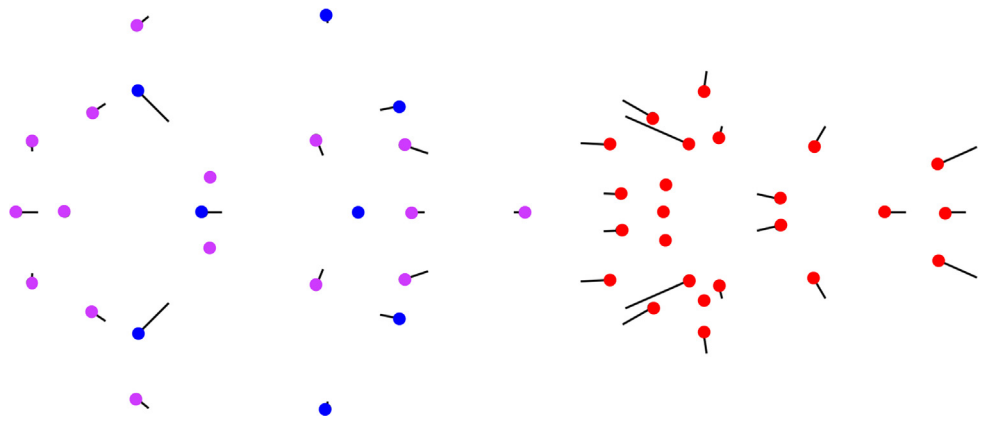

Fig. 5. Cranial shape changes associated with the major axis of variation (PC 1) in the principal components analysis (PCA) of female Han/Wistar and Long–Evans rats in the study sample. Lollipop graph of the shape changes that correspond to a positive change in the PC 1 score by 0.1 units. The colored circles show the landmark locations on the consensus configuration (face = red, vault = blue, base = purple) and the lines show the direction and magnitude of change in each landmark location.

Table 2
Mean and standard deviation (SD) values for centroid size (CS) values for the cranial modules of the face, vault, and base in female Han/Wistar and Long–Evans rats following TCDD exposure.

Dose TCDD (ng/kw bw/day)	Han/Wistar			Long–Evans		
	Face	Vault	Base	Face	Vault	Base
0	33.0 ± 0.6	22.4 ± 0.5	33.5 ± 0.5	35.1 ± 0.8	22.4 ± 0.2	33.7 ± 0.5
1	33.3 ± 1.0	22.8 ± 0.4	33.9 ± 0.6	35.2 ± 0.2	22.0 ± 0.2**	33.8 ± 0.4
10	32.9 ± 0.5	22.7 ± 0.3	33.6 ± 1.0	34.6 ± 0.4*	22.0 ± 0.2**	33.5 ± 0.2
100	32.8 ± 0.7	22.7 ± 0.4	33.8 ± 0.6	32.9 ± 0.4***	22.0 ± 0.2**	32.6 ± 0.3***
1000	31.8 ± 0.4***	22.4 ± 0.2	32.6 ± 0.3**	n/a	n/a	n/a

* Statistically significant difference from the control group at $p < 0.05$, Wilcoxon rank-sum test.
** Statistically significant difference from the control group at $p < 0.01$, Wilcoxon rank-sum test.
*** Statistically significant difference from the control group at $p < 0.001$, Wilcoxon rank-sum test.

Table 3
Results of benchmark dose modeling of centroid size (CS) values for the cranial modules of the face, vault, and base in female Han/Wistar and Long–Evans rats following TCDD exposure.

Dose TCDD (μg/kg bw)	Han/Wistar		Long–Evans		
	Face	Base	Face	Vault	Base
CED[a]	78.1	73.1	5.9	0	6.7
CED-L5[b]	59.2	53.5	5.1	0	5.6
CED/CED-L5[c]	1.3	1.4	1.2	1	1.2
Maximal Response (%)[d]	3.8	3.2	6.4	1.9	3.4

[a] Benchmark dose at a critical effect size (CES) of one standard deviation of the response in unexposed subjects.
[b] Lower bound of the confidence interval of the estimated CED.
[c] Ratio of CED/CED-L5 as a measure for uncertainty (a maximum of 10 is acceptable).
[d] Difference from background as a percentage derived from the fitted exponential model.

Table 4
Results of Spearman's rank correlation test for the relationship between centroid sizes for the cranial modules (face, vault, and base) and the overall centroid size and bodyweight gain during TCDD treatment (weeks 10–25), and femur, tibia length, and cross-sectional area in female Han/Wistar and Long–Evans rats.

	Han/Wistar			Long–Evans		
	Face	Vault	Base	Face	Vault	Base
Overall centroid size	0.90***	0.58***	0.90***	0.95***	0.32***	0.86***
Body weight gain	0.54***	0.37*	0.56***	0.80***	0.33*	0.74***
Femur length	0.60***	0.23	0.51***	0.65***	0.22	0.55***
Femur cross-sectional area	0.45**	0.17	0.49***	0.45**	0.37*	0.39**
Tibia length	0.69***	0.32*	0.67***	0.42*	−0.01	0.18
Tibia cross-sectional area	0.60***	0.37*	0.52***	0.72***	0.30	0.70***

* Statistically significant at $p < 0.05$.
** Statistically significant at $p < 0.01$.
*** Statistically significant at $p < 0.001$.

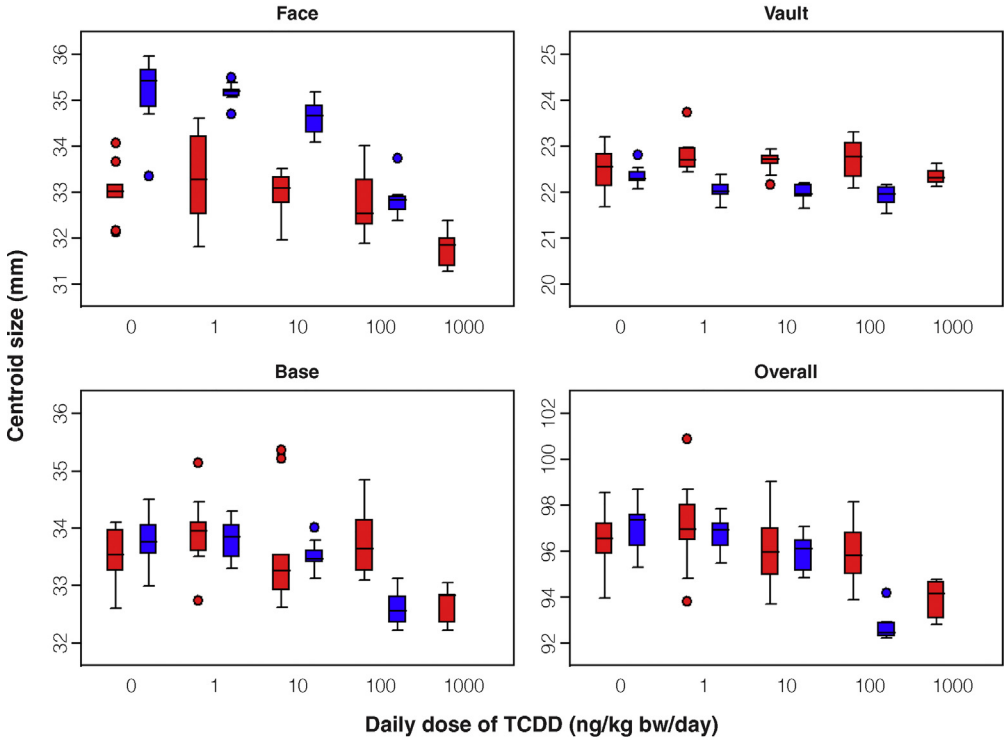

Fig. 6. Box plots of centroid size (CS) values for the three cranial modules and the overall cranium in female Han/Wistar and Long–Evans rats in the study sample. Boxes are color-coded by strain (Han/Wistar = red, Long–Evans = blue) and grouped by dose (0, 1, 10, 100, and 1000 ng/kg bw/day).

among strains (r_s = 0.86–0.90, $p < 0.001$). Both face and base CS values showed moderate to strong correlations with measurements of body weight gain during TCDD exposure (weeks 10–25) and posterior limb bone size (i.e., length and cross-sectional area of the femur and tibia) recorded in previous studies [11,26] (Table 4).

4. Discussion

This study demonstrates dose-dependent patterns of decreasing cranial size in TCDD-exposed rats. Compared to unexposed rats of the same strain, differences in CS values reached levels of high significance, suggesting that some of the exposed rats did not achieve their full genetic potential for cranial growth. In both strains, the greatest size reductions occurred within the highest dose groups, i.e., 1000 ng/kg bw/day in H/W rats and 100 ng/kg bw/day in L–E rats, consistent with reductions in length, cross-sectional area, and circumference of the femur, tibia, and lumbar vertebrae observed at the same exposure levels in other studies [11,12]. Furthermore, comparable to other studies showing about 10-fold greater sensitivity in L–E rats for decreased body weight [39] and reduced tibial length [11], the dose–response models for the face and base modules produced CED values that were about 10 times lower for the L–E rats (Table 3). These modules showed significant positive correlations with femoral and tibial size for both rat strains, and even stronger correlations with body weight gain during TCDD treatment (Table 4).

The cranial effects observed in the study sample reflect allometric patterning in the mammalian skeleton, which changes in proportions as it changes in size throughout ontogeny [40]. Comparative studies of skull growth in numerous different mammalian species have demonstrated that the vault follows a neural pattern of growth related to the expansion of the brain and the facial skeleton follows the somatic pattern of the postcranial skeleton, both of which are accommodated by an intermediate zone formed by the cranial base ([41]: 283). It is therefore not surprising that in this study the face shows the strongest correlations with limb bone size and the vault shows the weakest (Table 4). Taken together, these results suggest that the size reductions exhibited by the different cranial components of the TCDD-exposed rats may be caused by the systemic disruption of formative growth in the adult skeleton, rather than by actions specific or exclusive to the cranium. These findings are consistent with those reported in a previous experiment, where young adult H/W rats (i.e., 11–12 weeks old) were given a single dose of 1000 μg TCDD/kg and 6 weeks later showed different cranial proportions and lower body weight than the controls, in addition to perturbed tooth formation [16]. Concurrent decreases in head and body dimensions have also been observed in cortisone-treated male rats [42] and human infants exposed to AhR ligands such as polycyclic aromatic hydrocarbons (PAHs) [43] also see [58].

Among the three cranial modules analyzed, the facial skeleton exhibited the greatest magnitude size decrease in TCDD-exposed rats. Between the control and highest dose

groups, mean CS values for the face showed 3.6 and 6.3% decreases in H/W and L–E rats, compared to 2.7 and 3.2% decreases for the base, respectively (Table 2). These results demonstrate the importance of the timing of exposure as a factor in TCDD toxicity. Although the skeleton grows throughout life in most vertebrates, as new bone is added and old bone is removed in a continuous process of remodeling, the rates of growth related to adult bone formation change significantly across a short period of time. For the laboratory rat, whose average lifespan is 3 years, these changes occur within several weeks or months after birth [44]. In the neural growth pattern of the mammalian cranial vault, there is a rapid phase of enlargement in prenatal and early postnatal life and then relatively precious termination of growth in width before anteroposterior length [41]. Although the vault of the rat attains 93% of its adult size during the first month of life, the face exhibits significant growth until 5 months of age [45], specifically in the upper facial skeleton associated with the respiratory and alimentary tracts ([41]: 298). Thus, as rats and other mammals age, their faces become relatively elongated with respect to the cranial base and braincase ([46]: 1165). Moreover, the face of the young rat grows faster than the neurocranium, which it normally surpasses in anteroposterior length in female L–E rats at 60 days of age [47]. The stunted faces of these rats therefore can be attributed to the fact that exposure lasted for the entire period when the face becomes increasingly dominant in total skull length, i.e., from the second to the seventh months of life [47].

The mechanisms of growth by which cranial proportions change are essentially the same as those throughout the mammalian skeleton, and these processes can be altered or disrupted by a variety of internal and external forces [41]. Similar to our results, differential growth effects among the face, vault, and base have been observed in crania of rats that were malnourished during different ontogenetic periods [27]. Those malnourished during early development (i.e., from birth to weaning) showed the greatest size reduction in the vault, and when starvation continued until adulthood, the greatest size reduction was observed in the face [27]. In this study, it is therefore possible that decreased food consumption, as reflected in the dose-dependent decreases in body weight gain by the exposed rats, is the proximate cause of the observed cranial effects. Loss of body weight from hypophagia is a characteristic symptom of TCDD intoxication and appears to be the primary mechanism of TCDD lethality [48]. However, when TCDD-treated rats have been subjected to total parenteral nutrition, leading to an equal gain in body weight with control rats, no alleviating effect on TCDD lethality has been observed [49,50]. There thus appear to be numerous mechanisms of TCDD lethality, in addition to many sublethal and possibly inter-related mechanisms of TCDD toxicity, which remain to be fully understood [48].

Interspecific and intraspecific difference have been observed in rodent skeletal development with respect to the sequence of ossification [51], yet most comparisons of H/W and L–E strains have focused exclusively on their known genetic differences. In H/W rats, two point mutations in the gene for the AhR protein appear to provide the highest TCDD resistance of any laboratory animal [24,48]. However, as shown in this study, there are also intrinsic phenotypic differences in the skeletons of these two strains. Although the skulls of the control groups of H/W and L–E rats have cranial vaults and bases of comparable size, the face is 6.4% larger in L–E rats (Table 2, Fig. 5). This difference was relatively unaffected by low and medium TCDD exposure (resulting in 5.7 and 5.2% larger faces in L–E rats, respectively), but dropped close to unity at the highest exposure level for L–E rats (Table 2, Fig. 5). This change was due to a significant decrease in L–E face size (mean decrease = 1.7 mm, $p < 0.001$) without any significant decrease in H/W face size (Table 3, Fig. 6). At the highest exposure level for H/W rats, where TCDD doses were 10-fold greater than the highest exposure level for L–E rats, facial reduction was significant but less dramatic (mean decrease = 1.0 mm, $p < 0.001$).

The smaller decrease in H/W facial size is consistent with previous observations of H/W resistance to TCDD in numerous other endpoints. Nonetheless, it is well known that the impact of the altered AhR in H/W rats is endpoint-dependent, due to various combinations of downstream molecular pathways and biochemical processes [52]. Thus, the present results could also reflect lower growth potential in the H/W face related to its naturally smaller size. If L–E rats have a longer and/or later period of facial growth by comparison, during adulthood their faces may remain more susceptible to environmental stressors [53–55], which can alter natural between-strain differences in cranial shape [56]. Furthermore, although the H/W and L–E rats have different AhR alleles, five inbred strains of mice that possess the same AhR alleles have shown different TCDD-induced changes in mandibular size and shape [15]. These findings suggest that between-strain differences in TCDD responses may involve genes beyond the AhR locus, such as those that control the genetic architecture of a particular trait [15]. Consistent with these findings, our results suggest that genetically programmed differences in growth potential may modulate TCDD toxicity in different rat stains. Further research on H/W and L–E rats with *in utero* and lactational exposure to TCDD will help to clarify the role of these various factors of dioxin toxicity in the skull.

5. Conclusions

In this study, we show patterns of altered cranial form in H/W and L–E strains of female rats following long-term adult exposure to TCDD. Dose–response modeling of size variables for three cranial modules (face, vault, and base) produced considerably lower benchmark doses for the L–E rats, consistent with previous studies showing dioxin sensitivity by L–E rats in numerous aspects of somatic growth. The observed cranial patterns have significant correlations with TCDD-induced decreases in limb bone size and body weight gain, suggesting malnutrition as a proximate cause of these effects through the systematic disruption of adult skeletal formation. For both rat strains, the face showed greatest alterations by high doses of TCDD during the exposure period, when this part of the cranium is least mature and most sensitive to environmental stressors. However, the face was also the only cranial module that showed intrinsic size differences between these two rat strains.

Although H/W rats possess an altered AhR that appears to confer high dioxin resistance in a variety of endpoints, it is possible that the observed differences in facial reduction also reflect natural variation in allometry and ontogeny between H/W and L-E rats.

Acknowledgements

The authors thank Dr. Sebastian Wärmländer (Stockholm University) and John Ososky (National Museum of Natural History, Smithsonian Institution) for their help with sample preparations for this study, Yael Fitzpatrick for her assistance with the figures, and three anonymous reviewers for their helpful comments on the manuscript. This study was supported by the European Commission, DG XII (Contract No ENV4-CT96-0336) and the Academy of Finland, the Finnish Research Programme on Environmental Health (Project 42551).

Appendix A. Supplementary data

Supplementary data associated with this article can be found, in the online version, at doi:10.1016/j.toxrep.2014.12.007.

References

[1] K.C. Jones, P. de Voogt, Persistent organic pollutants (POPs): state of the science, Environ. Pollut. 100 (1999) 209–221.
[2] B.C. Kelly, M.G. Ikonomou, J.D. Blair, A.E. Morin, F.A. Gobas, Food web-specific biomagnification of persistent organic pollutants, Science 317 (2007) 236–239.
[3] D.C. Muir, R.J. Norstrom, M. Simon, Organochlorine contaminants in Arctic marine food chains: accumulation of specific polychlorinated biphenyls and chlordane-related compounds, Environ. Sci. Technol. 22 (1988) 1071–1079.
[4] F. Wania, D. Mackay, Tracking the distribution of persistent organic pollutants, Environ. Sci. Technol. 30 (1996) 390A–396A.
[5] Q. Qing Li, A. Loganath, Y. Seng Chong, J. Tan, J. Philip Obbard, Persistent organic pollutants and adverse health effects in humans, J. Toxicol. Environ. Health Part A 69 (2006) 1987–2005.
[6] Å. Bergman, J.J. Heindel, S. Jobling, K.A. Kidd, R.T. Zoeller (Eds.), The State-of-the-Science of Endocrine Erupting Chemicals—2012, UNEP/WHO, Geneva, 2013.
[7] M. Korkalainen, E. Kallio, A. Olkku, K. Nelo, J. Ilvesaro, J. Tuukkanen, A. Mahonen, M. Viluksela, Dioxins interfere with differentiation of osteoblasts and osteoclasts, Bone 44 (2009) 1134–1142.
[8] J.M. Martinez, M.J. DeVito, L.S. Birnbaum, N.J. Walker, Toxicology of dioxins and dioxinlike compounds, in: A. Schecter, T.A. Gasiewicz (Eds.), Dioxins and Health, 2nd ed., Wiley, Hoboken, 2003, pp. 137–157.
[9] M. Van den Berg, L. Birnbaum, A. Bosveld, B. Brunström, P. Cook, M. Feeley, J.P. Giesy, A. Hanberg, R. Hasegawa, S.W. Kennedy, Toxic equivalency factors (TEFs) for PCBs, PCDDs, PCDFs for humans and wildlife, Environ. Health Perspect. 106 (1998) 775.
[10] M. Herlin, M.A.J. Finnilä, P. Zioupos, A. Aula, J. Risteli, H.M. Miettinen, T. Jämsä, J. Tuukkanen, M. Korkalainen, H. Håkansson, M. Viluksela, New insights to the role of aryl hydrocarbon receptor in bone phenotype and in dioxin-induced modulation of bone microarchitecture and material properties, Toxicol. Appl. Pharmacol. 273 (2013) 219–226.
[11] M. Herlin, F. Kalantari, N. Stern, S. Sand, S. Larsson, M. Viluksela, J.T. Tuomisto, J. Tuomisto, J. Tuukkanen, T. Jämsä, Quantitative characterization of changes in bone geometry, mineral density and biomechanical properties in two rat strains with different Ah-receptor structures after long-term exposure to 2,3,7,8-tetrachlorodibenzo-*p*-dioxin, Toxicology 273 (2010) 1–11.
[12] T. Jämsä, M. Viluksela, J.T. Tuomisto, J. Tuomisto, J. Tuukkanen, Effects of 2,3,7,8-tetrachlorodibenzo-*p*-dioxin on bone in two rat strains with different aryl hydrocarbon receptor structures, J. Bone Miner. Res. 16 (2001) 1812–1820.
[13] H.M. Miettinen, P. Pulkkinen, T. Jämsä, J. Koistinen, U. Simanainen, J. Tuomisto, J. Tuukkanen, M. Viluksela, Effects of in utero and lactational TCDD exposure on bone development in differentially sensitive rat lines, Toxicol. Sci. 85 (2005) 1003–1012.
[14] D.E. Allen, L.J. Leamy, 2,3,7,8-Tetrachlorodibenzo-*p*-dioxin affects size and shape, but not asymmetry, of mandibles in mice, Ecotoxicology 10 (2001) 167–176.
[15] J.M. Keller, M.L. Zelditch, Y.M. Huet, L.J. Leamy, Genetic differences in sensitivity to alterations of mandible structure caused by the teratogen 2,3,7,8-tetrachlorodibenzo-*p*-dioxin, Toxicol. Pathol. 36 (2008) 1006–1013.
[16] S. Alaluusua, P.-L. Lukinmaa, R. Pohjanvirta, M. Unkila, J. Tuomisto, Exposure to 2,3,7,8-tetrachlorodibenzo-*para*-dioxin leads to defective dentin formation and pulpal perforation in rat incisor tooth, Toxicology 81 (1993) 1–13.
[17] H. Kattainen, J. Tuukkanen, U. Simanainen, J.T. Tuomisto, O. Kovero, P.-L. Lukinmaa, S. Alaluusua, J. Tuomisto, M. Viluksela, In utero lactational 2,3,7,8-tetrachlorodibenzo-*p*-dioxin exposure impairs molar tooth development in rats, Toxicol. Appl. Pharmacol. 174 (2001) 216–224.
[18] A. Kiukkonen, M. Viluksela, C. Sahlberg, S. Alaluusua, J.T. Tuomisto, J. Tuomisto, P.-L. Lukinmaa, Response of the incisor tooth to 2,3,7,8-tetrachlorodibenzo-*p*-dioxin in a dioxin-resistant and a dioxin-sensitive rat strain, Toxicol. Sci. 69 (2002) 482–489.
[19] H.M. Miettinen, R. Sorvari, S. Alaluusua, M. Murtomaa, J. Tuukkanen, M. Viluksela, The effect of perinatal TCDD exposure on caries susceptibility in rats, Toxicol. Sci. 91 (2006) 568–575.
[20] GuoF L., Y.-Y. Zhao, Y.-Y. Zhao, Z.-J. Sun, H. Liu, S.-l. Zhang, Toxic effects of TCDD on osteogenesis through altering IGFBP-6 gene expression in osteoblasts, Biol. Pharm. Bull. 30 (2007) 2018–2026.
[21] H. Jacobs, C. Dennefeld, B. Féret, M. Viluksela, H. Håkansson, M. Mark, N.B. Ghyselinck, Retinoic acid drives aryl hydrocarbon receptor expression and is instrumental to dioxin-induced toxicity during palate development, Environ. Health Perspect. 119 (2011) 1590.
[22] I. Yasuda, M. Yasuda, H. Sumida, H. Tsusaki, A. Arima, T. Ihara, S. Kubota, K. Asaoka, K. Tsuga, Y. Akagawa, In utero and lactational exposure to 2,3,7,8-tetrachlorodibenzo-*p*-dioxin (TCDD) affects tooth development in rhesus monkeys, Reprod. Toxicol. 20 (2005) 21–30.
[23] M. Yasuda, T. Sato, H. Sumida, Excencephalic mouse fetuses are resistant to cleft palate induction with 2,3,7,8-tetrachlorodibenzo-*p*-dioxin (TCDD), Teratology 43 (1991) 445.
[24] R. Pohjanvirta, J.M.Y. Wong, W. Li, P.A. Harper, J. Tuomisto, A.B. Okey, Point mutation in intron sequence causes altered carboxyl-terminal structure in the aryl hydrocarbon receptor of the most 2,3,7,8-tetrachlorodibenzo-*p*-dioxin-resistant rat strain, Mol. Pharmacol. 54 (1998) 86–93.
[25] J.T. Tuomisto, M. Viluksela, R. Pohjanvirta, J. Tuomisto, The AH receptor and a novel gene determine acute toxic responses to TCDD: segregation of the resistant alleles to different rat lines, Toxicol. Appl. Pharmacol. 155 (1999) 71–81.
[26] M. Viluksela, Y. Bager, J.T. Tuomisto, G. Scheu, M. Unkila, R. Pohjanvirta, S. Flodström, V.-M. Kosma, J. Mäki-Paakkanen, T. Vartiainen, Liver tumor-promoting activity of 2,3,7,8-tetrachlorodibenzo-*p*-dioxin (TCDD) in TCDD-sensitive and TCDD-resistant rat strains, Cancer Res. 60 (2000) 6911–6920.
[27] P.N. Gonzalez, E.E. Oyhenart, B. Hallgrímsson, Effects of environmental perturbations during postnatal development on the phenotypic integration of the skull, J. Exp. Zool. Part B 316 (2011) 547–561.
[28] S. Flodström, U. Ahlborg, Tumour promoting effects of 2,3,7,8-tetrachlorodibenzo-*p*-dioxin (TCDD)-effects of exposure duration, administration schedule and type of diet, Chemosphere 19 (1989) 779–783.
[29] F. Bookstein, Morphometric Tools for Landmark Data: Geometry and Biology, Cambridge University Press, Cambridge, 1991.
[30] B.D. Corner, S. Lele, J.T. Richtsmeier, Measuring precision of three-dimensional landmark data, J. Quant. Archaeol. 3 (1992) 347–359.
[31] A.H. Ross, S. Williams, Testing repeatability and error of coordinate landmark data acquired from crania, J. Forensic Sci. 53 (2008) 782–785.
[32] S. Sholts, L. Flores, P. Walker, S. Wärmländer, Comparison of coordinate measurement precision of different landmark types on human crania using a 3D laser scanner and a 3D digitiser: implications for applications of digital morphometrics, Int. J. Osteoarchaeol. 21 (2011) 535–543.
[33] N. von Cramon-Taubadel, B.C. Frazier, M. Mirazón Lahr, The problem of assessing landmark error in geometric morphometrics: Theory, methods, and modifications, Am. J. Phys. Anthropol. 134 (2007) 24–35.

[34] C.P. Klingenberg, MorphoJ: an integrated software package for geometric morphometrics, Mol. Ecol. Resour. 11 (2011) 353–357.
[35] H.A. Jamniczky, B. Hallgrímsson, Modularity in the skull and cranial vasculature of laboratory mice: implications for the evolution of complex phenotypes, Evol. Dev. 13 (2011) 28–37.
[36] C.P. Klingenberg, M. Barluenga, A. Meyer, Shape analysis of symmetric structures: quantifying variation among individuals and asymmetry, Evolution 56 (2002) 1909–1920.
[37] K. Crump, Critical issues in benchmark calculations from continuous data, Crit. Rev. Toxicol. 32 (2002) 133–153.
[38] W. Slob, Dose–response modeling of continuous endpoints, Toxicol. Sci. 66 (2002) 298–312.
[39] S. Sand, N. Fletcher, D.V. Rosen, F. Kalantari, M. Viluksela, J.T. Tuomisto, J. Tuomisto, A. Falk-Filipsson, H. Håkansson, Quantitative and statistical analysis of differences in sensitivity between Long–Evans and Han/Wistar rats following long-term exposure to 2,3,7,8-tetrachlorodibenzo-*p*-dioxin, Regul. Toxicol. Pharmacol. 57 (2010) 136–145.
[40] C.P. Klingenberg, Multivariate allometry, in: L.F. Marcus, M. Corti, A. Loy, G.J.P. Naylor, D.E. Slice (Eds.), Advances in Morphometrics, Plenum Press, New York, 1996, pp. 23–49.
[41] W. Moore, The Mammalian Skull, University of Cambridge Press, Cambridge, 1981.
[42] H. Che-Kuo, L.B. Johannessen, Skeletal changes in cortisone-treated male rats, J. Dent. Res. 49 (1970) 34–41.
[43] H. Choi, L. Wang, X. Lin, J.D. Spengler, F.P. Perera, Fetal window of vulnerability to airborne polycyclic aromatic hydrocarbons on proportional intrauterine growth restriction, Plos One 7 (2012) e35464.
[44] P. Sengupta, The laboratory rat: relating its age with human's, Int. J. Prev. Med. 4 (2013) 624.
[45] W. Moore, Skull growth in the albino rat (*Rattus norvegicus*), J. Zool. 149 (1966) 137–144.
[46] M.L. Zelditch, F.L. Bookstein, B.L. Lundrigan, Ontogeny of integrated skull growth in the cotton rat *Sigmodon fulviventer*, Evolution 46 (1992) 1164–1180.
[47] C.W. Asling, H.R. Frank, Roentgen cephalometric studies on skull development in rats. I. Normal and hypophysectomized females, Am. J. Phys. Anthropol. 21 (1963) 527–543.
[48] R. Pohjanvirta, J. Tuomisto, Short-term toxicity of 2,3,7,8-tetrachlorodibenzo-*p*-dioxin in laboratory animals: effects, mechanisms, and animal models, Pharmacol. Rev. 46 (1994) 483–549.
[49] T.A. Gasiewicz, M.A. Holscher, R.A. Neal, The effect of total parenteral nutrition on the toxicity of 2,3,7,8-tetrachlorodibenzo-*p*-dioxin in the rat, Toxicol. Appl. Pharmacol. 54 (1980) 469–488.
[50] C.-J. Huang Lu, R.B. Baggs, D. Redmond, E.C. Henry, A. Schecter, T.A. Gasiewicz, Toxicity and evidence for metabolic alterations in 2,3,7,8-tetrachlorodibenzo-*p*-dioxin-treated guinea pigs fed by total parenteral nutrition, Toxicol. Appl. Pharmacol. 84 (1986) 439–453.
[51] L.A.B. Wilson, C. Schradin, C. Mitgutsch, F.C. Galliari, A. Mess, M.R. Sánchez-Villagra, Skeletogenesis and sequence heterochrony in rodent evolution, with particular emphasis on the African striped mouse, *Rhabdomys pumilio* (Mammalia), Org. Divers. Evol. 10 (2010) 243–258.
[52] A.B. Okey, M.A. Franc, I.D. Moffat, N. Tijet, P.C. Boutros, M. Korkalainen, J. Tuomisto, R. Pohjanvirta, Toxicological implications of polymorphisms in receptors for xenobiotic chemicals: the case of the aryl hydrocarbon receptor, Toxicol. Appl. Pharmacol. 207 (2005) 43–51.
[53] G.S. Abed, P.H. Buschang, R. Taylor, R.J. Hinton, Maturational and functional related differences in rat craniofacial growth, Arch. Oral Biol. 52 (2007) 1018–1025.
[54] H.M. Pucciarelli, Growth of the functional components of the rat skull and its alteration by nutritional effects: a multivariate analysis, Am. J. Phys. Anthropol. 56 (1981) 33–41.
[55] J.R. Vandeberg, P.H. Buschang, R.J. Hinton, Craniofacial growth in growth hormone-deficient rats, Anat. Rec. Part A 278 (2004) 561–570.
[56] H.M. Pucciarelli, The effects of race, sex, and nutrition on craniofacial differentiation in rats: a multivariate analysis, Am. J. Phys. Anthropol. 53 (1980) 359–368.
[57] B.S. Vinogradov, A.I. Argiropulo, Key to Rodents, Israel Program for Scientific Translations, Jerusalem, 1968.
[58] S.K.T.S. Wärmländer, S.B. Sholts, J.M. Erlandson, T. Gjerdrum, R. Westerholm, Could the health decline of prehistoric California Indians be related to exposure to polycyclic aromatic hydrocarbons (PAHs) from natural bitumen? Environ. Health Perspect. 119 (2011) 1203.